Title	Apaf-1-dependent and independent cell death in mouse development
Author(s)	長坂, 明臣
Citation	大阪大学, 2009, 博士論文
Version Type	VoR
URL	https://hdl.handle.net/11094/592
rights	
Note	

Apaf-1-dependent and independent cell death in mouse development

(マウスの発生段階における **Apaf-1** 依存的細胞死と非依存的細胞死)

大阪大学大学院　生命機能研究科

時空生物学講座遺伝学研究室

指導教官　　長田　重一教授

長　坂　明　臣

(2009 年 3 月　修了)

Table of contents

General Introdution

Programmed cell death plays critical roles for many life phenomena such as animal homeostasis and development; its failure leads to malformation, autoimmune disease, and cancer. This is particularly evident in development, where cells must be eliminated in most animal tissues at specific times and places. Moreover, cell death can be classified into "apoptosis", "necrosis," and "autophagy," processes which are defined based on differences of appearance and/or enzymological aspects (Kroemer et al., 2009).

Apoptosis is accompanied by the condensation of nuclei, cytoplasm, and cell segmentation (Figure 1) while necrosis is characterized by gains in cell volume, swelling of organelles, and plasma membrane rupture (Figure 2). Furthermore, autophagy is accompanied by the sequestration of portions of the cytoplasm into autophagosomes, giving the cell a characteristic vacuolated appearance.
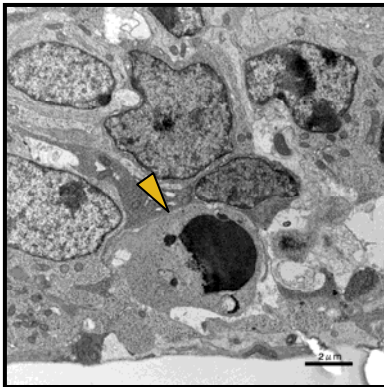
Figure 1: Apoptotic cell

The external granule cell layer of a cerebellum at P9. The yellow arrowhead indicates an apoptotic cell.
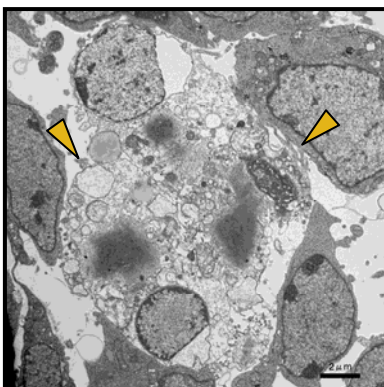
Figure 2: Necrotic cell

Necrotic cell in an E14.5 tail. The yellow arrowheads indicate necrotic cells.

Apoptotic signal transduction proceeds via two major pathways, one extrinsic and the other intrinsic. In the extrinsic pathway, signals from activated death receptors such as the Fas and TNF receptors trigger an initiator caspase (caspase 8) that activates a downstream effector caspase (mainly caspase 3) which in turn activates caspase-activated DNase (CAD) and causes the fragmentation of chromosomal DNA into nucleosomal units (Nagata, 2005). On the other hand, in the intrinsic pathway the cell death signals induce the release of cytochrome C from mitochondria via "BH3-only" proteins of the Bcl-2 family (Jiang and Wang, 2004; Strasser et al., 2000). Cytochrome C then activates apoptotic protease activating factor-1 (Apaf-1) which subsequently activates caspase 9, leading to the activation of caspase 3 and CAD.
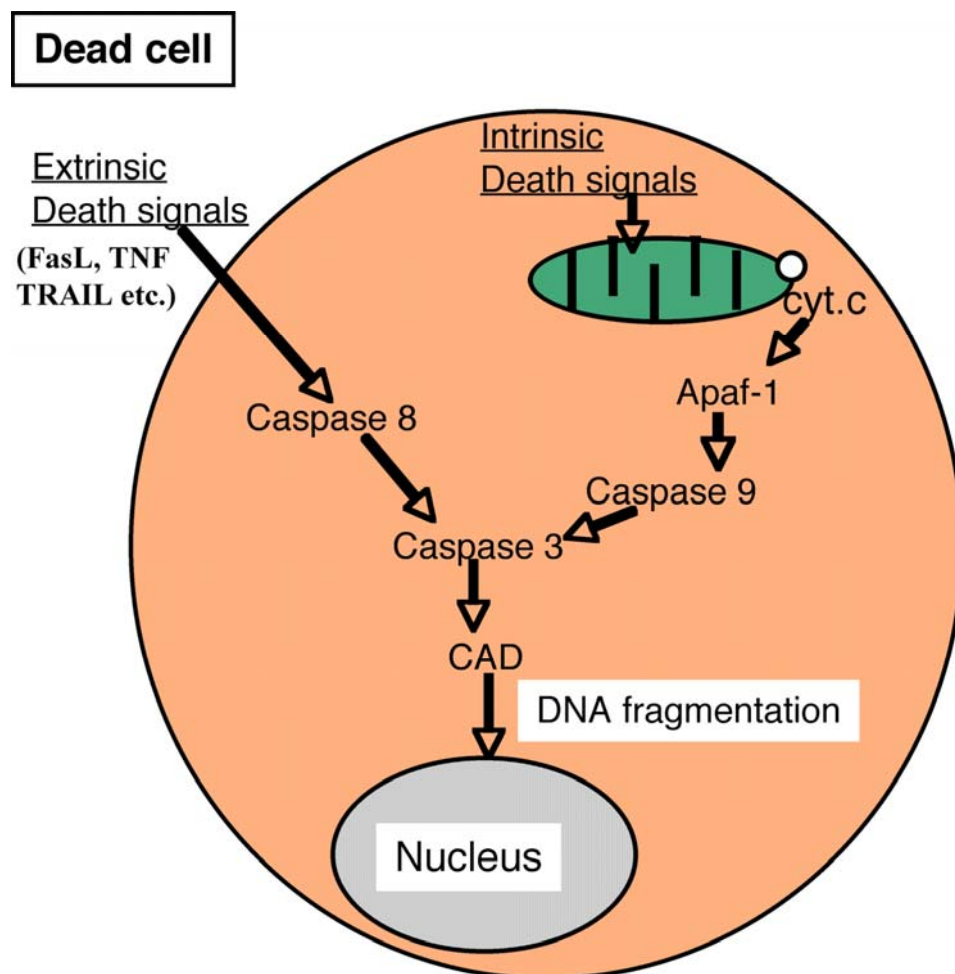

Figure 3: Apoptotic signal pathway (extrinsic and intrinsic pathways)

The role of the intrinsic apoptotic pathway in programmed cell death has been studied by establishing mice that lack genes involved in apoptotic signal transduction. But the results obtained with these knock-out mice are not always consistent. For example, Apaf-1 and caspase 9 are indispensable for cell death induced by cytotoxic agents or γ-radiation in various tissues, whereas lymphocytes undergo apoptosis without Apaf-1 or caspase 9 upon cytokine deprivation (Kuida et al., 1998; Marsden et al., 2002; Yoshida et al., 1998). Furthermore, except for craniofacial abnormalities and the hyperproliferation of neuronal cells, Apaf-1-deficient mice are apparently normal, especially in the C57BL/6 background suggesting that Apaf-1 does not play a critical role in mouse development (Okamoto et al., 2006).

Ineffective and toxic cells are generated during animal development and eliminated through programmed cell death, which is mainly mediated by apoptosis. But detection of apoptotic cells is difficult, because dying cells are swiftly engulfed and digested by phagocytes such as macrophages. As previously noted, one of the features of apoptotic cells is the fragmentation of chromosomal DNA, which is caused by CAD and DNase II. DNase II is responsible for digesting apoptotic DNA after phagocytes engulf them. Our laboratory reported that DNase II knock-out mice cannot digest DNA, so their macrophages in thymus and liver accumulate apoptotic nuclei (Figure 4)(Kawane et al., 2001; Kawane et al., 2003; Krieser et al., 2002). Therefore DNase II-deficient mice were used to detect the programmed cell death that occurs during mouse development. Apaf-1 deficient mice and DNase II deficient mice were crossed, and Apaf-1/DNase II double deficient mice were generated to examine whether or not programmed cell death during mouse development is Apaf-1 dependent. When cell death occurred in Apaf-1/DNaseII double deficient mice, nuclei were observed in dead cells carried by macrophages. On the other hand, when cell death did not occur in the mouse, then

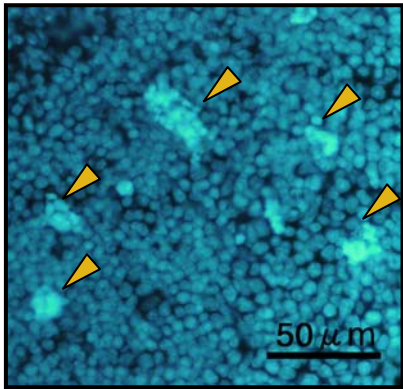nuclei were not observed in dead cells carried by macrophages (Figure 5).

Figure 4: E17.5 DNaseII knock-out thymus stained with DAPI. Yellow arrowheads show macrophages.
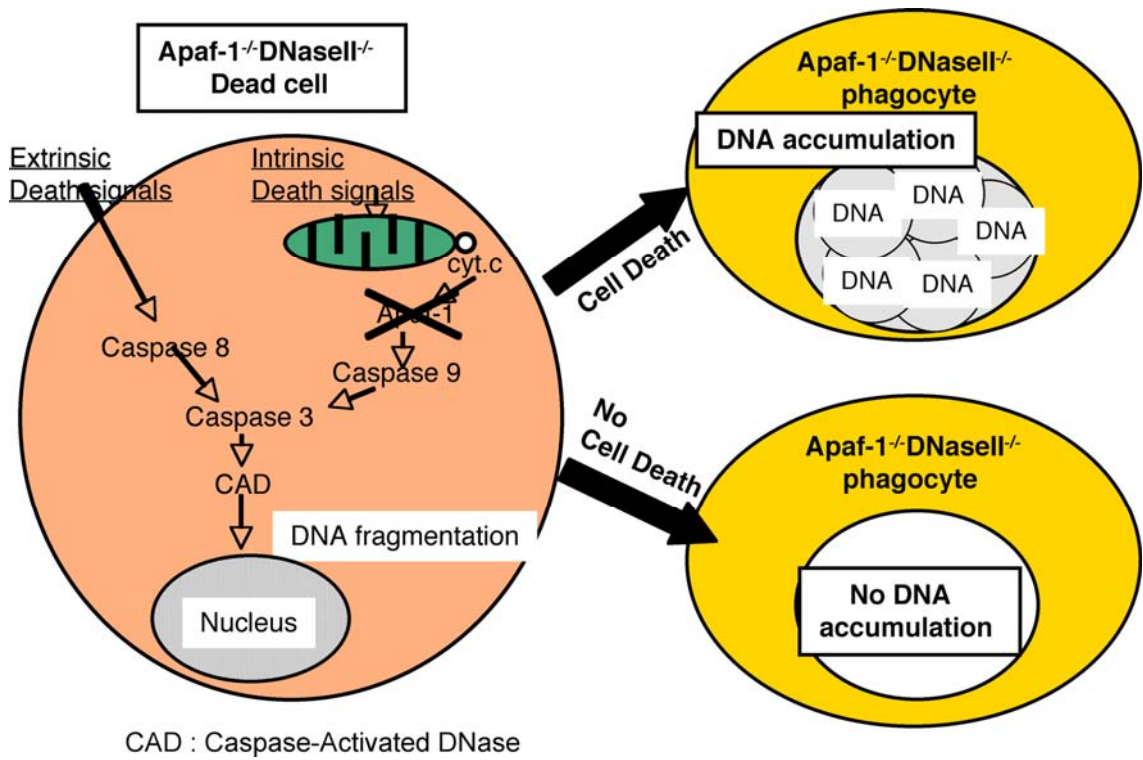

Figure 5: Generation of Apaf-1/DNaseII double knock-out mouse and detection of dead cells.

The analysis of Apaf-1/DNase II double deficient embryos indicates that cell death occurs as often in Apaf-1 deficient mice as wild type mice and caspase 3 was not activated in most tissues. Since DNA accumulating in macrophages was intact, cell death occurs in a caspase/CAD independent manner in Apaf-1 deficient mice. Exceptionally, caspase 3 was activated in E14.5 Apaf-1/DNase II double deficient thymus, indicating that the cells died by Apaf-1-independent apoptosis. Many necrotic cells were found in the Apaf-1 knock-out embryos except in E14.5 thymus, suggesting that Apaf-1-independent programmed cell death occurred via necrosis, and the necrotic cells were engulfed by macrophages.

Necrosis has traditionally been considered an accidental and uncontrolled form of cell death, but it has recently been reported that necrosis is regulated by signal transduction (Festjens et al., 2006). Furthermore, necrotic cells were observed in caspase 9 or Apaf-1 knock-out mice (Chautan et al., 1999) where apoptosis occurs in the wild type. Several mediators, cellular processes, and organelles are implicated in necrotic cell death but it is still unclear how they interrelate with each other.

These results suggest programmed cell death during mouse development can occur via Apaf-1 independent-apoptosis or necrosis, even in Apaf-1 deficient cases.

Reference

Chautan, M., G. Chazal, F. Cecconi, P. Gruss, and P. Golstein. 1999. Interdigital cell death can occur through a necrotic and caspase-independent pathway. *Curr. Biol.* 9:967-70.

Festjens, N., T. Vanden Berghe, and P. Vandenabeele. 2006. Necrosis, a well-orchestrated form of cell demise: signalling cascades, important mediators and concomitant immune response. *Biochim Biophys Acta.* 1757:1371-87.

Jiang, X., and X. Wang. 2004. Cytochrome C-mediated apoptosis. *Annu. Rev. Biochem.* 73:87-106.

Kawane, K., H. Fukuyama, G. Kondoh, J. Takeda, Y. Ohsawa, Y. Uchiyama, and S. Nagata. 2001. Requirement of DNase II for definitive erythropoiesis in the mouse fetal liver. *Science.* 292:1546-1549.

Kawane, K., H. Fukuyama, H. Yoshida, H. Nagase, Y. Ohsawa, Y. Uchiyama, T. Iida, K. Okada, and S. Nagata. 2003. Impaired thymic development in mouse embryos deficient in apoptotic DNA degradation. *Nat. Immunol.* 4:138-144.

Krieser, R.J., K.S. MacLea, D.S. Longnecker, J.L. Fields, S. Fiering, and A. Eastman. 2002. Deoxyribonuclease IIa is required during the phagocytic phase of apoptosis and its loss causes lethality. *Cell Death Differ.* 9:956-962.

Kroemer, G., L. Galluzzi, P. Vandenabeele, J. Abrams, E.S. Alnemri, E.H. Baehrecke, M.V. Blagosklonny, W.S. El-Deiry, P. Golstein, D.R. Green, M. Hengartner, R.A. Knight, S. Kumar, S.A. Lipton, W. Malorni, G. Nunez, M.E. Peter, J. Tschopp, J. Yuan, M. Piacentini, B. Zhivotovsky,

and G. Melino. 2009. Classification of cell death: recommendations of the Nomenclature Committee on Cell Death 2009. *Cell Death Differ*. 16:3-11.

Kuida, K., T.F. Haydar, C.Y. Kuan, Y. Gu, C. Taya, H. Karasuyama, M.S. Su, P. Rakic, and R.A. Flavell. 1998. Reduced apoptosis and cytochrome c-mediated caspase activation in mice lacking caspase 9. *Cell*. 94:325-337.

Marsden, V.S., L. O'Connor, L.A. O'Reilly, J. Silke, D. Metcalf, P.G. Ekert, D.C. Huang, F. Cecconi, K. Kuida, K.J. Tomaselli, S. Roy, D.W. Nicholson, D.L. Vaux, P. Bouillet, J.M. Adams, and A. Strasser. 2002. Apoptosis initiated by Bcl-2-regulated caspase activation independently of the cytochrome c/Apaf-1/caspase-9 apoptosome. *Nature*. 419:634-7.

Nagata, S. 2005. DNA degradation in development and programmed cell death. *Annu. Rev. Immunol.* 23:853-75.

Okamoto, H., H. Shiraishi, and H. Yoshida. 2006. Histological analyses of normally grown, fertile Apaf1-deficient mice. *Cell Death Differ*. 13:668-71.

Strasser, A., L. O'Connor, and V.M. Dixit. 2000. Apoptosis signaling. *Annu. Rev. Biochem.* 69:217-45.

Yoshida, H., Y.Y. Kong, R. Yoshida, A.J. Elia, A. Hakem, R. Hakem, J.M. Penninger, and T.W. Mak. 1998. Apaf1 is required for mitochondrial pathways of apoptosis and brain development. *Cell*. 94:739-750.

Abstract

Many cells die during mammalian development and are engulfed by macrophages. Macrophages carrying engulfed DNA are present in *DNase II*$^{-/-}$ embryos, providing a system for studying programmed cell death during mouse development. Here, we showed that an *Apaf-1*-null mutation in the *DNase II*$^{-/-}$ embryos greatly reduced the number of macrophages carrying DNA at E11.5. At later stages of the embryogenesis (E14.5-E17.5), dead cells were engulfed in an *Apaf-1*-independent manner. Caspase 3 was activated in E14.5 thymus of *Apaf-1*$^{-/-}$*DNase II*$^{-/-}$ embryos, indicating that the cells died by an *Apaf-1*-independent apoptosis. No processed caspase 3 was detected in other tissues and the E17.5 thymus of *Apaf-1*$^{-/-}$*DNase II*$^{-/-}$ embryos, and the DNA accumulated in the macrophages appeared intact. Many necrotic cells were found in the tail of the *Apaf-1*$^{-/-}$ embryos, suggesting that the *Apaf-1*-independent programmed cell death occurred *via* necrosis, and the necrotic cells were engulfed by macrophages. Thus, Apaf-1 appears dispensable for programmed cell death in mouse development, which is backed-up by Apaf-1-independent systems.

Introduction

Many useless and toxic cells are generated during animal development and removed by programmed cell death, which is mainly mediated by apoptosis (Jacobson et al., 1997; Vaux and Korsmeyer, 1999). Apoptosis is accompanied by morphological changes, such as the blebbing and condensation of cells, loss of membrane symmetry, and nuclear condensation (Kerr et al., 1972). Late in apoptosis, dying cells are fragmented into small "apoptotic bodies," which are recognized by phagocytes for engulfment. This morphological change in the cells and their rapid disposal are distinct from necrosis, in which cells swell, the plasma membranes are ruptured, and the cellular contents are believed to be released.

The signal transduction involved in apoptotic cell death has been intensively studied (Adams, 2003; Danial and Korsmeyer, 2004) and shown to proceed by two major pathways, an extrinsic and an intrinsic one. In the extrinsic pathway, signals from death receptors, such as Fas and TNF receptor, activate an initiator caspase, caspase 8, that activates downstream effector caspases, mainly caspase 3, leading to the cleavage of more than 300 cellular proteins (Nagata, 1997). One of the caspase 3 substrates is the inhibitor of caspase activated DNase (CAD), and its cleavage by caspase 3 inactivates the ability to associate with CAD, allowing CAD to cause the fragmentation of chromosomal DNA into nucleosomal units (Nagata, 2005). In the intrinsic pathway, death signals cause the release of cytochrome C from mitochondria *via* "BH3-only" proteins of the Bcl-2 family (Jiang and Wang, 2004; Strasser et al., 2000). The cytochrome C binds to Apaf-1 and activates caspase 9, which leads to the activation of caspase 3 and CAD, resulting in the cleavage of cellular substrates and the fragmentation of chromosomal DNA. Apoptotic cells that die by either the intrinsic or extrinsic pathway expose phosphatidylserine on their surface (Fadok et al., 1998).

Macrophages and immature dendritic cells recognize the phosphatidylserine and rapidly engulf the apoptotic cells (Ravichandran and Lorenz, 2007). The engulfed dead cells are transferred to lysosomes, where all their components are degraded.

The role of the intrinsic apoptotic pathway in programmed cell death has been studied by establishing mice that lack genes involved in apoptotic signal transduction (Cecconi et al., 1998; Hao et al., 2005; Kuida et al., 1998; Lindsten et al., 2000; Yoshida et al., 1998). The results obtained with these knock-out mice have not always been consistent among groups. For example, Yoshida et al. (1998) and Kuida et al. (1998) reported that Apaf-1 and caspase 9 are indispensable for the cell death induced by cytotoxic agents or γ-radiation in various tissues, whereas Marsden et al. (2002) reported that lymphocytes undergo apoptosis without Apaf-1 or caspase 9 upon cytokine deprivation. Furthermore, except for craniofacial abnormalities and the hyperproliferation of neuronal cells, *Apaf-1*-deficient mice are apparently normal, especially in the C57BL/6 background (Okamoto et al., 2006), suggesting Apaf-1 does not play a critical role in mouse development.

Since dying cells are swiftly engulfed and degraded by macrophages, the detection of apoptotic cells in animals is not an easy task. DNase II is responsible for digesting the DNA of apoptotic cells after macrophages engulf them, and many macrophages carrying undigested DNA are present in *DNase II*-deficient embryos (Kawane et al., 2001; Kawane et al., 2003; Krieser et al., 2002). Here, we used *DNase II*-deficient mice to detect the programmed cell death that occurs during mouse development. The analysis of *Apaf-1-* and *DNase II*-double deficient embryos indicated that Apaf-1 was dispensable for this process. In the thymus of *Apaf-1$^{-/-}$* embryos at E14.5, caspases were activated in an Apaf-1-independent manner. In most other tissues, cells also died by an Apaf-1-independent mechanism, but probably *via* the necrotic pathway, and were

engulfed by macrophages. These results indicate that Apaf-1-independent systems function as a back-up system for the programmed cell death in mammalian development.

Results

Apaf-1-dependent apoptosis in mouse embryos at E11.5

We detected apoptotic cells by TUNEL staining. The TUNEL staining of E11.5 wild-type mouse embryos yielded barely detectable signals (data not shown). A mutation of *nuc-1*, a homolog of *DNase II*, enhances the TUNEL-positivity in *C. elegans* (Wu et al., 2000). Similarly, the mouse *DNase II*$^{-/-}$ embryos showed very strong TUNEL signals (Fig. 1A).

TUNEL-positive spots were frequent in several regions, such as the diencephalon at the cerebrum, the lamina terminalis, somites and mesonephric ducts. Observations at higher magnification showed TUNEL-positivity in these regions was at least 10 times stronger in the *DNase II*$^{-/-}$ than the wild-type embryos. The TUNEL-positive spots in the *DNase II*$^{-/-}$ embryos were clustered into foci that were positive for DAPI (Fig. 2). The foci were located inside F4/80-positive macrophages, suggesting that they were the DNA of engulfed apoptotic cells. The engulfment of corpses in *C. elegans* requires the activation of caspase; a mutation in *Ced-3* or *Ced-4*, homologues of caspase and Apaf-1, respectively, prevents the engulfment of cell corpses (Reddien and Horvitz, 2004). Accordingly, a null-mutation of *Apaf-1* blocked the generation of TUNEL-positive foci (Fig. 1B and 2), indicating that the apoptotic cell death and engulfment of dead cells in the E11.5 mouse embryos were apparently Apaf-1-dependent.
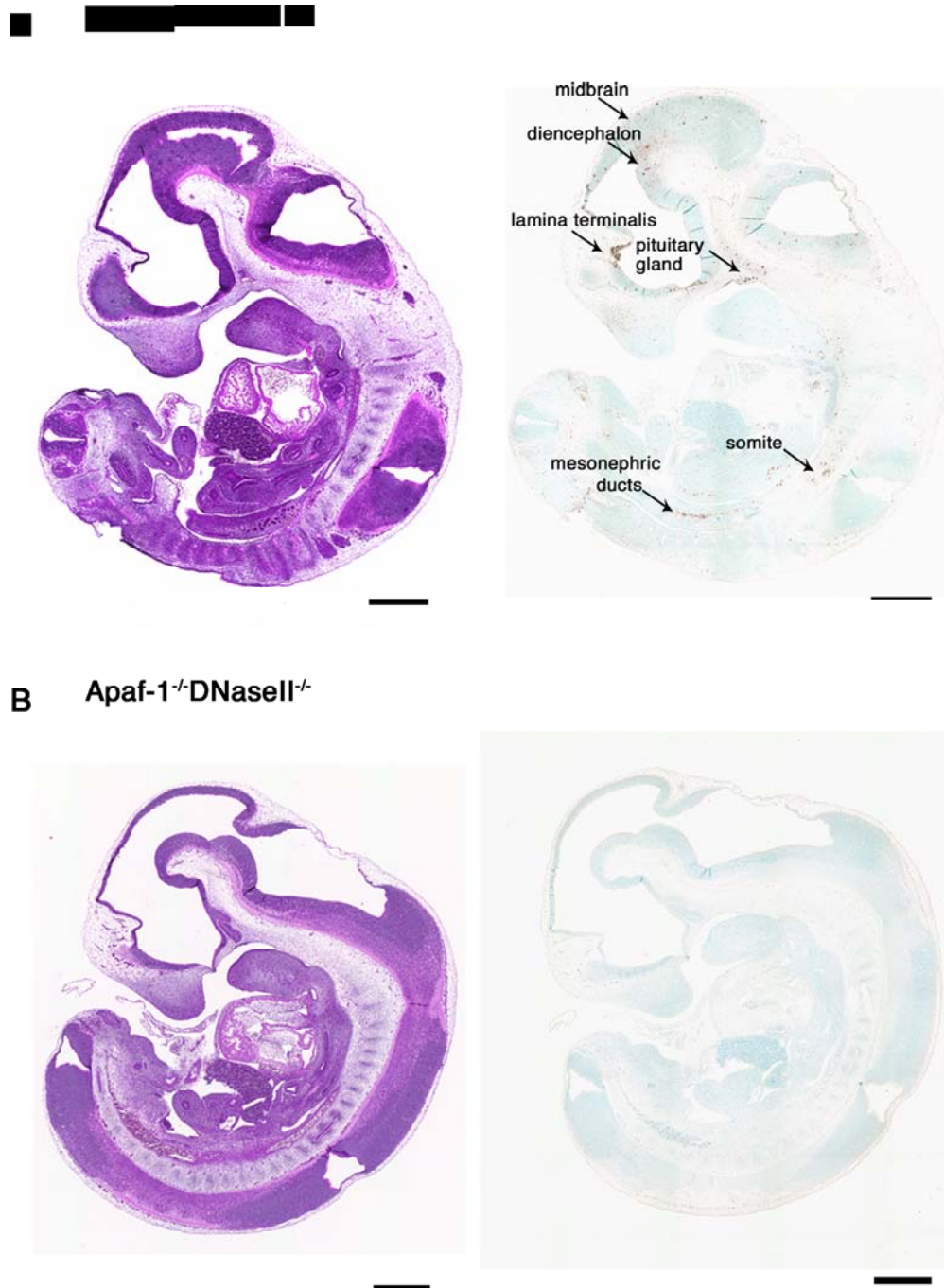
14

Figure 1. Apaf-1-dependent TUNEL-positive cells in *DNase II^-/-* mouse embryos.

Adjacent paraffin sections from E11.5 *Apaf-1^+/-DNase II^-/-* (A) and *Apaf-1^-/-DNase II^-/-* (B) whole embryos were stained with hematoxylin-eosin (left) or with TUNEL, followed by counter-staining with methyl green (right). Scale Bar, 500 μm.
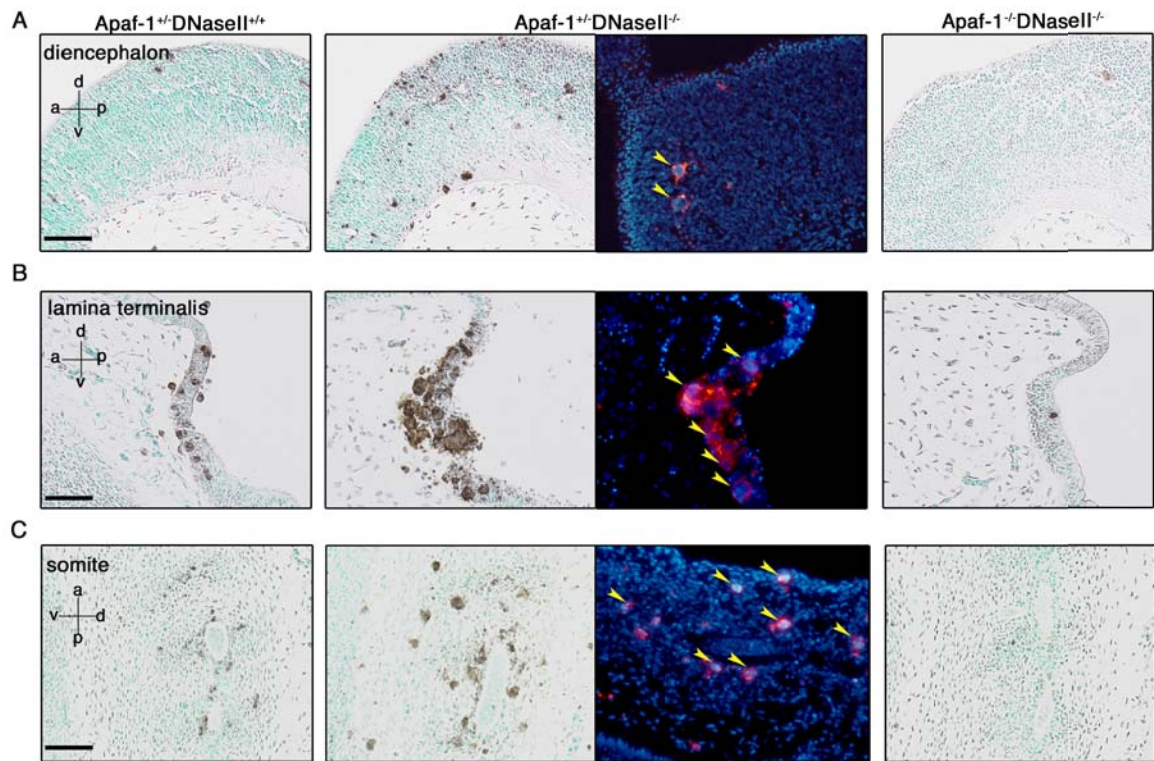
Figure 2. Apaf-1-dependent engulfment of TUNEL-positive cells in *DNase II$^{-/-}$* mouse embryos. Paraffin sections of the diencephalon (A), lamina terminalis (B), and somites (C) from E11.5 *Apaf-1$^{+/-}$DNase II$^{+/+}$*, *Apaf-1$^{+/-}$DNase II$^{-/-}$*, and *Apaf-1$^{-/-}$DNase II$^{-/-}$* embryos, were stained with TUNEL using the digoxigenin/anti-digoxigenin peroxidase system and DAB-chromogenic substrate, counter-stained with methyl green, and observed by microscopy. Cryosections from E11.5 *Apaf-1$^{+/-}$DNase II$^{-/-}$* mouse embryos were stained with DAPI and a rat mAb against mouse F4/80, followed by incubation with peroxidase-conjugated rabbit anti-rat IgG, and detected by Cy3-labelled tyramide. The staining profiles with DAPI and anti-F4/80 are merged, and shown in the middle panels. Polarity of the embryos is indicated in left panels. a, anterior; p, posterior; d, dorsal; v, ventral. Yellow arrowheads indicate the macrophages carrying undigested DNA. Scale Bar, 100 μm.

Apaf-1-dependent and -independent cell death in mouse embryos at E14.5

Many TUNEL-positive foci were also observed throughout the *DNase II$^{-/-}$* embryos at E14.5 (data not shown). *DNase II$^{-/-}$* embryos produce IFNβ which is lethal, but the lethality can be rescued by a deficiency of *IFN type I receptor* (Yoshida et al., 2005). To exclude the possible cell death caused by IFNβ, the TUNEL-staining was carried out with the *DNase II$^{-/-}$IFN-IR$^{-/-}$* embryos, and many TUNEL-positive foci could be detected in various tissues (Fig. 3A and 3B). The null-mutation of *Apaf-1* blocked the generation of TUNEL-positive foci in most tissues of the E14.5 *DNase II$^{-/-}$IFN-IR$^{-/-}$* embryos (Fig. 3A and 3B). For example, many TUNEL-positive foci were present at the interdigits of the hind paw of *DNase II$^{-/-}$IFN-IR$^{-/-}$* embryos, and activated caspase 3 could be detected in this region. The deficiency of *Apaf-1* prevented both the caspase activation and the appearance of TUNEL-positive foci. Probably due to the inhibition of apoptotic cell death, the formation of interdigits was retarded in the *Apaf-1$^{-/-}$DNase II$^{-/-}$IFN-IR$^{-/-}$* embryos compared with *Apaf-1$^{+/+}$DNase II$^{-/-}$IFN-IR$^{-/-}$* embryos, as reported for *Apaf-1*-null mice (Yoshida et al., 1998).

Many TUNEL- and DAPI-positive foci were observed in the thymus of *DNase II$^{-/-}$IFN-IR$^{-/-}$* embryos at E14.5 (Fig. 3C). In contrast to the interdigits, the TUNEL-positive foci were present in the *Apaf-1$^{-/-}$* thymus as well, where processed caspase 3 was also detected (Fig. 3C). Electron microscopy indicated that the DAPI-positive material in the E14.5 thymus was inside macrophages, and the DNA that accumulated in the macrophages was fragmented in both the *Apaf-1$^{+/+}$* and *Apaf-1$^{-/-}$* thymus (Fig. 3D). These results indicated that the thymocytes at E14.5 could activate caspase 3 and CAD using an Apaf-1-independent mechanism.
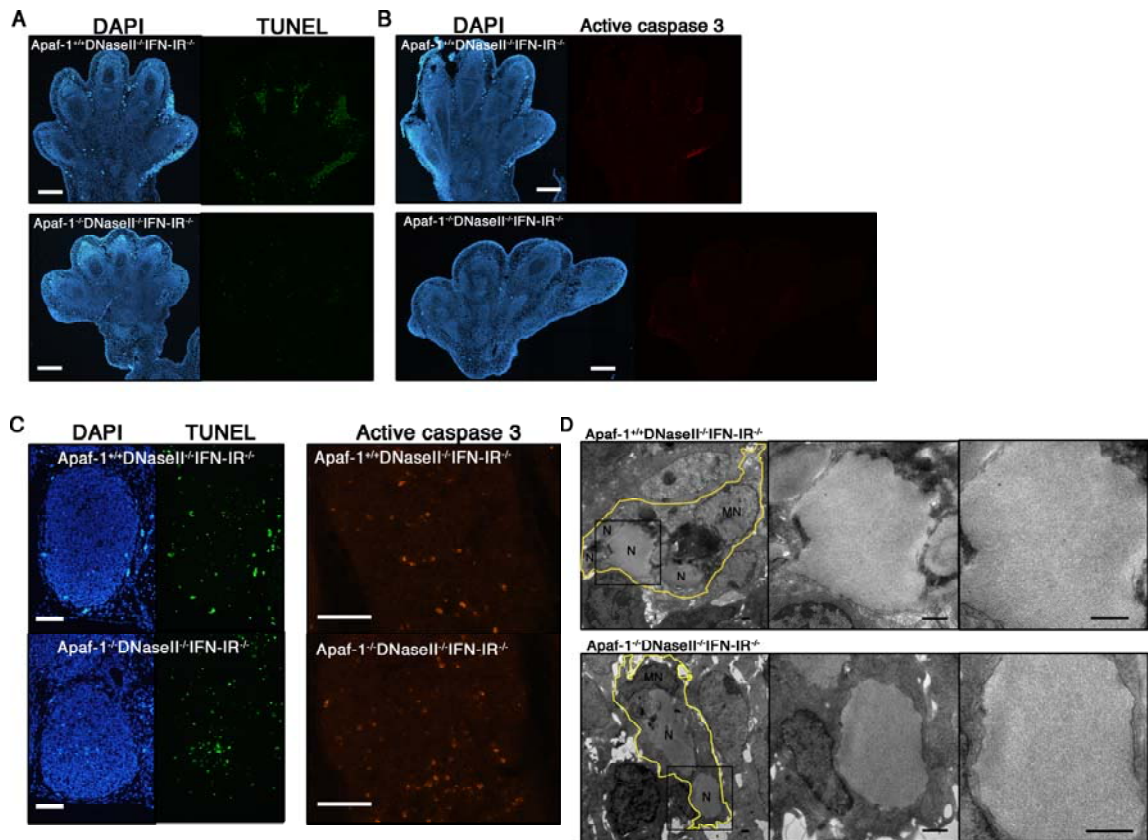
Figure 3. Programmed cell death in E14.5 embryos. Paraffin sections (A) or cryosections (B) of the hind paws from E14.5 $Apaf$-$1^{+/+}DNase\ II^{-/-}IFN$-$IR^{-/-}$ (upper panels) and $Apaf$-$1^{-/-}DNase\ II^{-/-}IFN$-$IR^{-/-}$ (lower panels) embryos were stained with DAPI and TUNEL (A), or with DAPI and an anti-processed caspase 3 mAb (B). Scale bar, 100 μm. (C) Paraffin sections (left panels) or cryosections (right panel) of the thymus from E14.5 $Apaf$-$1^{+/+}DNase\ II^{-/-}IFN$-$IR^{-/-}$ (upper panels) and $Apaf$-$1^{-/-}DNase\ II^{-/-}IFN$-$IR^{-/-}$ (lower panels) embryos were stained with DAPI and TUNEL using the digoxigenin/anti-digoxigenin Fluoresein system (left panels), or with an anti-processe caspase 3 mAb (right panels). Scale bars, 100 μm. (D) Sections from the thymus of E14.5 $Apaf$-$1^{+/+}DNase\ II^{-/-}IFN$-$IR^{-/-}$ (upper panels) and $Apaf$-$1^{-/-}DNase\ II^{-/-}IFN$-$IR^{-/-}$ (lower panels) embryos were analyzed by electron microscopy. Boxed areas were enlarged. N, nuclear DNA from the engulfed dead cells. Scale bar, 1 μm.

Apaf-1-independent programmed cell death in E17.5 embryos

Fewer DAPI-positive foci were detected in the *Apaf-1$^{+/+}$DNase II$^{-/-}$IFN-IR$^{-/-}$* embryos at E17.5 than at E14.5, as seen, for example, in the interdigits (Fig. 4A), which have completely formed by E17.5. On the other hand, the interdigits of the *Apaf-1$^{-/-}$DNase II$^{-/-}$IFN-IR$^{-/-}$* embryos carried more DAPI-positive foci at E17.5 than at E14.5 (Fig. 4A). As found in the *Apaf-1$^{+/+}$* embryos, the DAPI-positive material in the *Apaf-1$^{-/-}$* embryos was located within F4/80-positive macrophages (Fig. 4B). Electron microscopy, however, showed that unlike the DNA accumulated in the *Apaf-1$^{+/+}$* embryos, the DNA in the macrophages at the interdigits of the E17.5 *Apaf-1$^{-/-}$DNase II$^{-/-}$IFN-IR$^{-/-}$* embryos was apparently intact (Fig. 4C). These results suggested that in late embryogenesis, the cells in the interdigits could die in an Apaf-1-independent manner, and the dead cells were engulfed by macrophages.
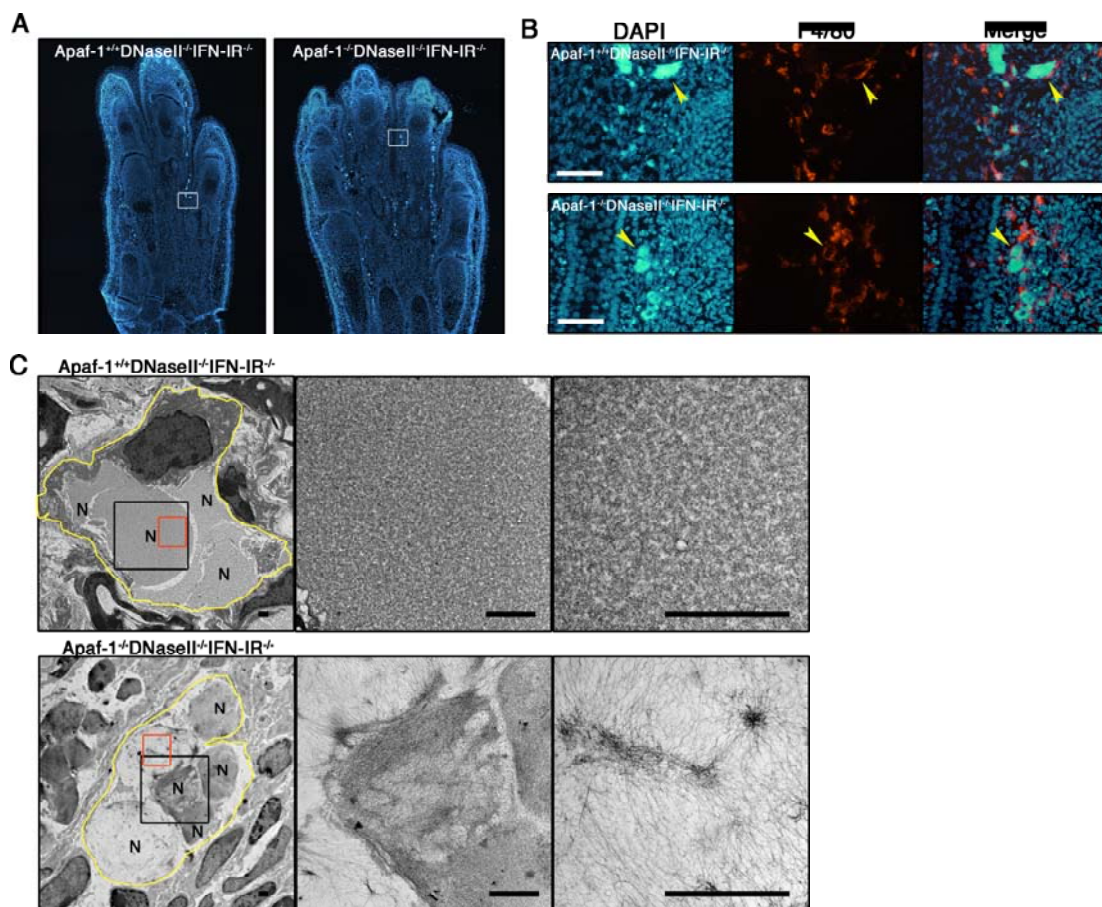
Figure 4. Apaf-1-independent engulfment of dead cells in the hind paws at E17.5. (A) Cryosections of the hind paws from E17.5 *Apaf-1*$^{+/+}$*DNase II*$^{-/-}$*IFN-IR*$^{-/-}$ (left panel) and *Apaf-1*$^{-/-}$*DNase II*$^{-/-}$*IFN-IR*$^{-/-}$ (right panel) embryos were stained with DAPI. (B) Sections from E17.5 *Apaf-1*$^{+/+}$*DNase II*$^{-/-}$*IFN-IR*$^{-/-}$ (upper panels) and *Apaf-1*$^{-/-}$*DNase II*$^{-/-}$*IFN-IR*$^{-/-}$ (lower panels) mouse embryos were stained with DAPI and a rat mAb against mouse F4/80, followed by incubation with peroxidase-conjugated rabbit anti-rat IgG, and detected by Cy3-labelled tyramide. The staining profiles with DAPI and anti-F4/80 are merged in the right panels. Arrowheads indicate macrophages carrying engulfed DNA. DAPI stainig of figures in B were white boxes in A. Scale bars, 50 μm. (C) Sections from the E17.5 hind paws of *Apaf-1*$^{+/+}$*DNase II*$^{-/-}$*IFN-IR*$^{-/-}$ (upper panels) and *Apaf-1*$^{-/-}$*DNase II*$^{-/-}$*IFN-IR*$^{-/-}$ (lower panels) mice were analyzed by electron microscopy. Macrophages are indicated by yellow lines. The areas surrounded by black and red boxes are enlarged in the middle and right panels. N, nuclear DNA from the engulfed dead cells; MN, macrophage nuclei. Scale bar, 1 μm.

Apaf-1-independent non-apoptotic programmed cell death was also observed in the thymus at E17.5. That is, both the *Apaf-1*$^{+/+}$ and *Apaf-1*$^{-/-}$ thymus of *DNase II*$^{-/-}$*IFN-IR*$^{-/-}$ embryos carried DAPI-positive foci (Fig. 5A). The DAPI-positive foci in the E17.5 *Apaf-1*$^{+/+}$ thymus were TUNEL-positive. However, the TUNEL-reactivity of the foci in the E17.5 *Apaf-1*$^{-/-}$*DNase II*$^{-/-}$*IFN-IR*$^{-/-}$ thymus was very weak, and processed caspase 3 was barely detected, confirming that CAD-mediated DNA fragmentation could not occur without Apaf-1. The DAPI-positive foci in the *Apaf-1*$^{-/-}$ thymus were inside macrophages, and the DNA that accumulated in the macrophages was intact (Fig. 5B). These properties of the E17.5 Apaf-1$^{-/-}$ thymus were different from those of the E14.5 thymus, in which caspase 3 was activated in an Apaf-1-independent manner (Fig. 3C).
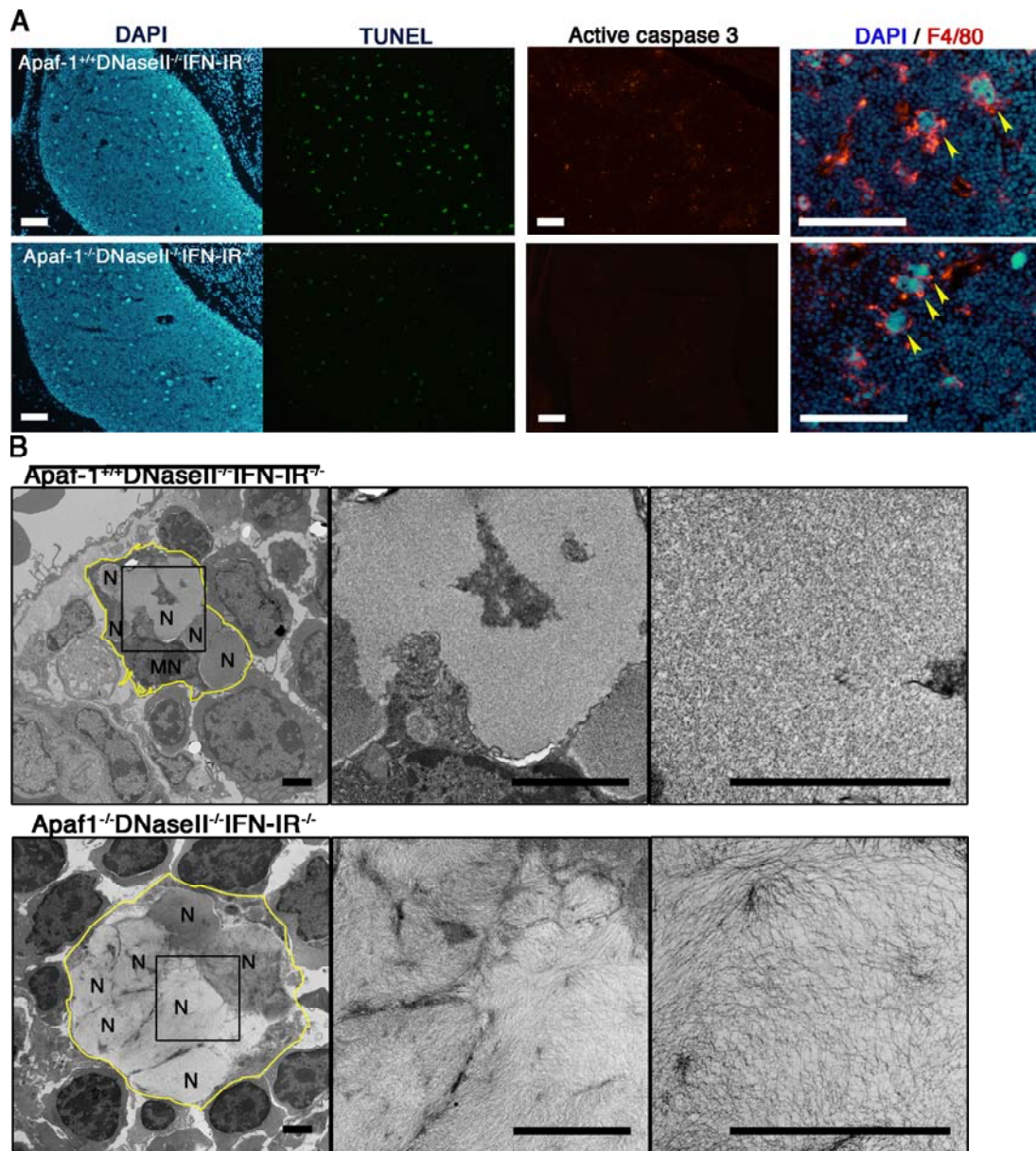
Figure 5. Apaf-1- independent engulfment of dead cells in the E17.5 thymus. (A) Adjacent cryosections of the thymus from E17.5 embryos with *Apaf-1^{+/+}DNase II^{-/-}IFN-IR^{-/-}* (upper panels) and *Apaf-1^{-/-}DNase II^{-/-}IFN-IR^{-/-}* (lower panels) embryos were stained with DAPI and TUNEL using the digoxigenin/anti-digoxigenin Fluorescein system (left panels), or with an anti-processed caspase 3 mAb (middle panel). Scale bars, 100 μm. In the right panel, the sections were stained with DAPI and a rat mAb against mouse F4/80, followed by incubation with peroxidase-conjugated rabbit anti-rat IgG, and detected by Cy3-labelled tyramide. The

21

staining profiles with DAPI and anti-F4/80 were merged. Yellow arrowheads indicate the macrophages carrying engulfed DNA. Scale bar, 100 μm. (B) Sections from the E17.5 thymus of *Apaf-1$^{+/+}$DNase II$^{-/-}$IFN-IR$^{-/-}$* (upper panels) and *Apaf-1$^{-/-}$DNase II$^{-/-}$IFN-IR$^{-/-}$* (lower panels) embryos were analyzed by electron microscopy. Boxed areas in the left panels were enlarged in the adjacent right panels. N, nuclear DNA from the engulfed dead cells; MN, macrophage nuclei. Scale bars, 2 μm.

Apaf-1-independent necrosis-like cell death

At the ventral ectodermal ridge of the tail in mouse embryos, many cells undergo programmed cell death, which was detected as DAPI-positive foci in the *DNase II$^{-/-}$IFN-IR$^{-/-}$* embryos at E14.5 (Fig. 6A and B). Similar to the E17.5 interdigits and thymus, both *Apaf-1$^{+/+}$* and *Apaf-1$^{-/-}$* embryos showed DAPI-positive foci in the ectodermal ridge. In the *Apaf-1$^{+/+}$* embryos, the DNA that accumulated in the ridge was TUNEL-positive, and many processed-caspase 3-positive cells could also be detected in this region. On the other hand, the DNA that accumulated in the *Apaf-1$^{-/-}$* embryos was TUNEL-negative, and processed-caspase 3-positive cells were hardly detectable. Since the DAPI-positive foci were relatively closely clustered in the ventral ectodermal ridge of the tail (Fig. 6C), we analyzed this region by electron microscopy. As shown in Fig. 6D, many unengulfed, dying cells with characteristics of necrosis were detected in the E14.5 *Apaf-1$^{-/-}$* embryos. That is, the unengulfed dying cells showed mottled chromatin condensation, nuclear membrane detachment and rupture, and dilated mitochondria. Approximately 5% of the cells in the tail ridge of E14.5 *Apaf-1$^{-/-}$* embryos had the necrosis-like morphology (Fig. 6E), but apoptotic dying cells were hardly detectable. Necrotic cells in the tail ridge of *Apaf-1$^{+/+}$* embryos were rare, about 1%, but cells with apoptotic characteristics, such as condensed and fragmented nuclei, were relatively

abundant (1.72%). These results indicated that the cells in the tail ridge underwent necrosis in the absence of Apaf-1, and that these dead cells were engulfed by macrophages.
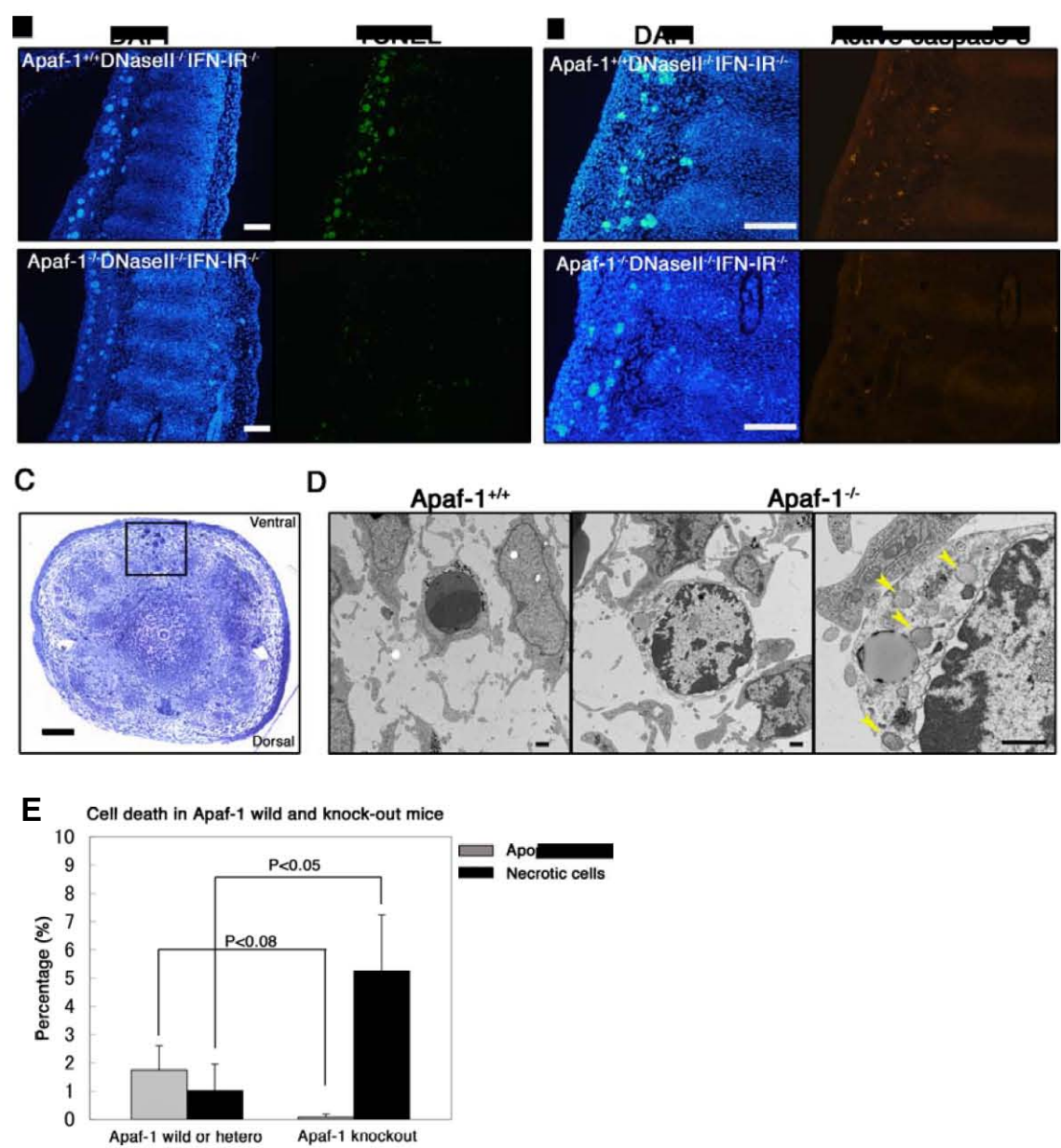
Figure 6. Apaf-1-independent necrosis-like cell death in the tails at E14.5. Paraffin sections (A) or cryosections (B) of the tail from E14.5 *Apaf-1$^{+/+}$DNase II$^{-/-}$IFN-IR$^{-/-}$* (upper panels) and *Apaf-1$^{-/-}$DNase II$^{-/-}$IFN-IR$^{-/-}$* (lower panels) embryos were stained with DAPI and TUNEL (A), and with DAPI and a rabbit mAb against processed caspase 3 (B). Scale bar, 100 μm. (C) A transverse section of the tail from an *Apaf-1$^{+/-}$DNase II$^{-/-}$IFN-IR$^{-/-}$* embryo at E14.5 was stained with toluidine blue. Scale bars, 100 μm. (D) Sections from the E14.5 tail of *Apaf-1$^{+/+}$DNase II$^{+/-}$IFN-IR$^{-/-}$* (left panel) and *Apaf-1$^{-/-}$DNase II$^{+/+}$IFN-IR$^{-/-}$* (middle and right panels) embryos were analyzed by electron microscopy. Apoptotic cells in the *Apaf-1$^{+/+}$* embryos (left panel) and necrotic cells (middle and right panels) in the *Apaf-1$^{-/-}$* embryos are shown. Arrowheads indicate dilated mitochondria. Scale bar, 1 μm. (E) Increase in necrotic cells in the *Apaf-1$^{-/-}$* tail. Electron micrographs (55 x 55 μm) with low magnification of the ventral parts (boxed area in C) of the tail of *Apaf-1$^{+/+}$* or $^{+/-}$ and *Apaf-1$^{-/-}$* embryos at E14.5 were assembled, and the percentages of apoptotic and necrotic cells out of 950 cells were determined. Average numbers obtained from three embryos are plotted. Welch's *t*-test was used to test for difference, *P* values are shown.

Discussion

Many cells die during mammalian development. However, since the dead cells are swiftly engulfed by macrophages for degradation, it is difficult to detect them. For example, more than 90% of thymocytes undergo programmed cell death during the development of the thymus. However, only a small percentage of the cells can be stained by TUNEL at a given time point (Surh and Sprent, 1994). Many neurons also undergo programmed cell death in the brain, but the reported number differs greatly among researchers (Blaschke et al., 1996; Thomaidou et al., 1997; Verney et al., 2000), probably due to the difficulty in detecting dead cells that are quickly eliminated. Here, we used *DNase II*-null mice to detect the programmed cell death that occurs during mouse embryogenesis. The *DNase II*-null mice carried in various tissues macrophages that contained undigested DNA, suggesting that cells died surrounding the macrophages and were engulfed. Although it is difficult to determine which and how many cells died, the *DNase II*$^{-/-}$ mice were nonetheless useful for localizing the regions where programmed cell death occurs. The macrophages carrying undigested DNA eventually disappeared, probably because those with a heavy load of DNA could not survive, suggesting that the *DNase II*$^{-/-}$ mice can also be used to estimate the time when programmed cell death takes place. In fact, we have been able to show that specific layers of cerebral neurons undergo programmed cell death at specific stages of mouse embryogenesis (A.N., K.K., and S.N., manuscript in preparation).

Crossing the *Apaf-1*$^{-/-}$ mice with *DNase II*$^{-/-}$ mice, we showed that most of the apoptotic cell death during mouse embryonic development takes place *via* an Apaf-1-dependent pathway. This agrees with previous reports that deletion of the *Apaf-1* or *caspase 9* gene blocks apoptotic cell death in the brain, ear, and thymus (Kuida et al., 1998; Yoshida et al., 1998).

Most of the thymocytes at the later stage of embryogenesis, E17.5, are CD4$^+$CD8$^+$, and they undergo negative or positive selection. Our results suggest that this selection process takes place *via* Apaf-1-dependent apoptosis or Apaf-1-independent necrosis (see below). On the other hand, very surprisingly, we found that caspase 3 could be activated in an Apaf-1-independent manner in the E14.5 thymus. Most thymocytes at E14.5 are CD4$^-$CD8$^-$ (Rodewald et al., 1992). At this stage in the thymus, not only thymocytes, but also macrophages, dendritic cells, and epithelial cells are growing vigorously, and they may undergo programmed cell death. The Fas system induces apoptosis by an Apaf-1-independent mechanism (Nagata, 1997). However, the Fas-deficient *lpr* mutation had no effect on the TUNEL-positive cells in the thymus of E14.5 mice (A.N. and S.N., data not shown), suggesting that Fas-induced apoptosis is not responsible for the programmed cell death in the E14.5 thymus. The finding that thymocytes could undergo Apaf-1-independent apoptosis may be consistent with reports that hemopoietic cells reconstituted with fetal liver cells can activate caspase without Apaf-1 (Hara et al., 2002; Marsden et al., 2002; Matsuki et al., 2002). To understand this apoptosis, it will be necessary to determine how the caspases are activated without Apaf-1, and it will be interesting to learn if other cells undergo Apaf-1-independent apoptosis.

Even when the caspase-dependent apoptotic cell death was blocked in *Apaf-1*-deficient mice, macrophages carrying undigested DNA were present in the embryo, in particular at the late stage of development, indicating that cells could die without Apaf-1. Several Apaf-1- or caspase-independent cell death processes have been proposed, including autophagic cell death and necrosis (Kroemer et al., 2009). As reported for the interdigits of *Apaf-1$^{-/-}$* embryos (Chautan et al., 1999), we found in the ectodermal ridge of the tails of *Apaf-1$^{-/-}$* mice many cells exhibiting the characteristics of necrosis, but no cells with the characteristics of autophagy (double-membraned

vacuoles). One possible cause of necrotic cell death is that the stimuli that induce programmed cell death in mouse embryogenesis cause cytochrome C to be released, inactivating mitochondrial function, which leads to cell death. The mice lacking both Bak and Bax that are essential for the release of cytochrome C (Wei et al., 2001), show the persistence of interdigital webs (Lindsten et al., 2000), which suggests that Bak/Bax can cause necrotic cell death by releasing cytochrome C. It will be interesting to examine whether the null mutation of *Bax* and *Bak* can prevent the generation of macrophages carrying undigested DNA in *DNase II*-null embryos.

In *Apaf-1$^{-/-}$* embryos, dead cells were found in macrophages, indicating that the necrotic cells were recognized by macrophages for engulfment. In *C. elegans*, a common set of genes mediates the removal of both apoptotic and necrotic cell corpses (Chung et al., 2000). On the other hand, different mechanisms have been proposed to clear apoptotic and necrotic cells in mammalian system (Krysko et al., 2006). Apoptotic cells expose phosphatidylserine, which is recognized by specific receptors or opsonins for engulfment (Ravichandran and Lorenz, 2007). Since necrotic cells also expose phosphatidylserine at a late stage (Kroemer et al., 2009), it is possible that similar receptors or opsonins mediate the engulfment of apoptotic and necrotic cells. The complement system is another candidate for the engulfment of late apoptotic or necrotic cells (Zwart et al., 2004). It will be interesting to study the engulfment of necrotic cells by crossing the *Apaf-1$^{-/-}$* mice with mice deficient in the engulfment of apoptotic or necrotic cells (Botto et al., 1998; Hanayama et al., 2004). Unengulfed apoptotic cells are difficult to find in mouse tissues. On the other hand, we frequently detected unengulfed dead cells with necrotic morphology in the *Apaf-1$^{-/-}$* embryos, suggesting that the engulfment of necrotic cells is inefficient compared with that of apoptotic cells. This may allow noxious materials to be released from dying cells. In addition, the

engulfment of necrotic cells but not apoptotic ones is known to cause the release of inflammatory cytokines (Fadok et al., 2001). In this regard, it will be interesting to study whether the normally developing $Apaf-1^{-/-}$ mice suffer from inflammatory disease.

Materials and Methods

Mice

C57BL/6 mice were purchased from Nippon SLC. *DNase II$^{-/-}$* mice (Kawane et al., 2001) were backcrossed to C57BL/6 at lease six times. *IFN-IR$^{-/-}$* mice (Muller et al., 1994) in the C57BL/6 background were obtained from Dr. Michel Aguet (Swiss Institute for Experimental Cancer Research, Epalinges, Switzerland). *Apaf-1$^{-/-}$* mice in the C57BL/6 background were described previously (Okamoto et al., 2006; Yoshida et al., 1998). *DNase II$^{-/-}$IFN-IR$^{-/-}$* mice and *Apaf-1$^{-/-}$DNase II$^{-/-}$IFN-IR$^{-/-}$* embryos were generated by crossing *Apaf-1$^{+/-}$DNase II$^{-/-}$IFN-IR$^{-/-}$* parents, respectively. Mice were housed in specific pathogen-free facilities at Osaka University Medical School and Oriental Bio Service. All animal experiments were conducted according to the Guidelines for Animal Experiments of Osaka University or Kyoto University. To determine the genotype of *DNase II* and *IFN-IR* alleles, DNA was prepared from embryonic tissues or adult tail-snip tissue, as described (Laird et al., 1991), and was analyzed by PCR. For the *DNase II* gene, a sense primer specific for the wild-type (5'-GCCCATCTAGACTAACTTTC-3') or mutant allele (5'-GATTCGCAGCGCATCGCCTT-3'; sequence in the neomycin-resistance gene) was used with a common antisense primer (5'-GAGTCTTAGTCCTTTGCTCCG-3'). The wild-type and mutant alleles for *IFN-IR* were examined with a wild-type (5'-AAGATGTGCTGTTCCCTTCCTCTGCTCTGA-3') or mutant-specific (5'-CCTGCGTGCAATCCATCTTG-3') antisense primer and a common sense primer (5'-ATTATTAAAAGAAAAGACGAGGCGAAGTGG-3'). For the *Apaf-1* allele, a wild-type (5'-CTCAAACACCTCCTACAA-3') or mutant-specific (5'-GTCATCTGGAAGGGCAGCGA-3') antisense primer was used with a common sense primer (5'-GGGCCAGCTCATTCCTC-3').

Histochemical analysis with paraffin sections

Embryos were fixed with 4% PFA in 0.1 M Na-phosphate buffer (pH 7.2) containing 4% sucrose at 4°C for more than one day with shaking. They were gradually dehydrated by dipping into 50, 70, 80, and 90% ethanol at room temperature for 12 h each, and then twice in 100% ethanol for 1 h. The samples were soaked twice in 100% xylene at room temperature for 1 h, in a 1:1 mixture of xylene and paraffin for 2 h at 60°C. They were embedded in paraffin by successive incubations in paraffin for 12 h and 4 h at 60°C, and sectioned at 4 μm using a microtome (RM2245, Leica).

For hematoxylin-eosin staining, sections were deparaffinized by dipping three times into xylene for 5 min each, hydrated by dipping into a graded series (100, 100, 95, 70, 50, and 30%) of ethanol for 3-5 min each, and into H_2O for 5 min. They were then incubated for 5 min with 0.1% (w/v) hematoxylin, washed with H_2O, and stained with 0.11% (w/v) eosin. After washing with H_2O, they were dehydrated by dipping into 70, 80, 90, and 100% ethanol for 1-3 min each, and washed three times with xylene for 5 min each.

For TUNEL staining, sections were treated at room temperature for 20 min with 20 μg/ml Proteinase K, and stained with an Apoptag kit (Millipore), according to the manufacturer's instructions, except that the amount of terminal transferase was reduced to 10% of the recommended concentration. Sections were mounted with Mount-Quick (Daido Sangyo) or Fluormount (Diagnostic Biosystems), and observed by fluorescence microscopy (IX-70, Olympus, or BioRevo BZ-9000, Keyence).

Histochemical analysis with cryosections

Embryos were fixed at 4°C in 4% PFA containing 4% sucrose in 0.1 M Na-phosphate buffer (pH 7.2) for 2 h, successively immersed in 10% and 20% sucrose-containing 0.1

M Na-phosphate buffer (pH 7.2) for 4 h and overnight each, embedded in O.C.T compound (Sakura Finetek), and frozen in liquid nitrogen. Sections (10 μm) were prepared using a cryostat (CM3050 S, Leica) in the cold (-16°C to -25°C).

To detect active caspase 3, sections were fixed with 4% PFA in PBS at room temperature for 10 min, and blocked with 5% normal goat serum in PBS containing 0.3% Triton X-100 at room temperature for 1 h. They were then stained at 4°C overnight with a 100-fold-diluted rabbit mAb against active caspase 3 (Cell Signaling), followed by incubation at room temperature for 1 h with Cy3-conjugated goat anti-rabbit IgG (Jackson Laboratories).

For the staining of F4/80 antigen, a rat hybridoma against mouse F4/80 (Austyn and Gordon, 1981) was grown in serum-free GIT medium (Nippon Pharmaceutical). Cryosections from mouse embryos were fixed at room temperature for 10 min with 1% PFA in PBS. After blocking with 10% normal rabbit serum and 0.5% BSA in PBS at room temperature for 1 h, sections were incubated at 4°C overnight with the supernatant of the F4/80 hybridoma, and washed with PBS containing 0.5% BSA. The endogenous peroxidase was quenched by incubation at 4°C for 20-30 min with 3% H_2O_2 in methanol, and incubated at room temperature for 45 min with peroxidase-conjugated rabbit anti-rat IgG (Dako). The signals were detected by incubation at room temperature for 5 min with Cy3-labelled tyramide (PerkinElmer).

TUNEL staining was performed as described above, except that the concentration of terminal transferase was reduced to 0.4-0.5% of that recommended by the manufacturer. Sections were mounted with mounting reagent containing 1-2 μg/ml DAPI (Dojin Laboratories), and observed by microscopy as described above.

Electron microscopy

Embryonic tissues were fixed by incubation at 4°C for 2 h in 0.1 M Na-phosphate buffer (pH 7.2) containing 2% PFA and 2% glutaraldehyde. After being washed 5 times with 0.1 M Na-phosphate buffer (pH 7.2) at 4°C for 20 min each, the samples were post-fixed at 4°C for 2 h with 1% OsO_4 in the same buffer, and dehydrated at 4°C by dipping into a graded series (50, 60, 70, 80, 90, 99%) of ethanol for 10 min each. After two 20-min immersions in 100% ethanol, the samples were incubated at 35°C twice in propylene oxide for 20 min, in a 3:1 mixture of propylene oxide and epoxide for 1 h, in a 1:3 mixture of propylene oxide and epoxide for 1 h, and in epoxide overnight. They were then embedded in epoxide by incubation at 60°C for 3 days. Ultrathin sections (80-90 nm) were prepared with an ultramicrotome (Ultracut N, Reichert-Nissei), stained with uranyl acetate and lead citrate, and observed with a Hitachi H-7650 microscope.

Acknowledgements

Abbreviations: CAD, caspase-activated DNase.

References

Adams, J.M. 2003. Ways of dying: multiple pathways to apoptosis. *Genes Dev.*
17:2481-95.

Austyn, J.M., and S. Gordon. 1981. F4/80, a monoclonal antibody directed
specifically against the mouse macrophage. *Eur. J. Immunol.*
11:805-815.

Blaschke, A.J., K. Staley, and J. Chun. 1996. Widespread programmed cell
death in proliferative and postmitotic regions of the fetal cerebral
cortex. *Development.* 122:1165-74.

Botto, M., C. Dell'Agnola, A.E. Bygrave, E.M. Thompson, H.T. Cook, F. Petry,
M. Loos, P.P. Pandolfi, and M.J. Walport. 1998. Homozygous C1q
deficiency causes glomerulonephritis associated with multiple
apoptotic bodies. *Nat. Genet.* 19:56-59.

Cecconi, F., G. Alvarez-Bolado, B.I. Meyer, K.A. Roth, and P. Gruss. 1998.
Apaf1 (CED-4 homolog) regulates programmed cell death in
mammalian development. *Cell.* 94:727-737.

Chautan, M., G. Chazal, F. Cecconi, P. Gruss, and P. Golstein. 1999.
Interdigital cell death can occur through a necrotic and
caspase-independent pathway. *Curr. Biol.* 9:967-70.

Chung, S., T.L. Gumienny, M.O. Hengartner, and M. Driscoll. 2000. A
common set of engulfment genes mediates removal of both apoptotic
and necrotic cell corpses in C. elegans. *Nat. Cell Biol.* 2:931-7.

Danial, N.N., and S.J. Korsmeyer. 2004. Cell death: critical control points.
Cell. 116:205-19.

Fadok, V.A., D.L. Bratton, S.C. Frasch, M.L. Warner, and P.M. Henson. 1998. The role of phosphatidylserine in recognition of apoptotic cells by phagocytes. *Cell Death & Differ.* 5:551-562.

Fadok, V.A., D.L. Bratton, L. Guthrie, and P.M. Henson. 2001. Differential effects of apoptotic versus lysed cells on macrophage production of cytokines: role of proteases. *J. Immunol.* 166:6847-54.

Hanayama, R., M. Tanaka, K. Miyasaka, K. Aozasa, M. Koike, Y. Uchiyama, and S. Nagata. 2004. Autoimmune disease and impaired uptake of apoptotic cells in MFG-E8-deficient mice. *Science.* 304:1147-50.

Hao, Z., G.S. Duncan, C.C. Chang, A. Elia, M. Fang, A. Wakeham, H. Okada, T. Calzascia, Y. Jang, A. You-Ten, W.C. Yeh, P. Ohashi, X. Wang, and T.W. Mak. 2005. Specific ablation of the apoptotic functions of cytochrome C reveals a differential requirement for cytochrome C and Apaf-1 in apoptosis. *Cell.* 121:579-91.

Hara, H., A. Takeda, M. Takeuchi, A.C. Wakeham, A. Itie, M. Sasaki, T.W. Mak, A. Yoshimura, K. Nomoto, and H. Yoshida. 2002. The apoptotic protease-activating factor 1-mediated pathway of apoptosis is dispensable for negative selection of thymocytes. *J. Immunol.* 168:2288-95.

Jacobson, M.D., M. Weil, and M.C. Raff. 1997. Programmed cell death in animal development. *Cell.* 88:347-354.

Jiang, X., and X. Wang. 2004. Cytochrome C-mediated apoptosis. *Annu. Rev. Biochem.* 73:87-106.

Kawane, K., H. Fukuyama, G. Kondoh, J. Takeda, Y. Ohsawa, Y. Uchiyama, and S. Nagata. 2001. Requirement of DNase II for definitive

erythropoiesis in the mouse fetal liver. *Science*. 292:1546-1549.

Kawane, K., H. Fukuyama, H. Yoshida, H. Nagase, Y. Ohsawa, Y. Uchiyama, T. Iida, K. Okada, and S. Nagata. 2003. Impaired thymic development in mouse embryos deficient in apoptotic DNA degradation. *Nat. Immunol.* 4:138-144.

Kerr, J.F., A.H. Wyllie, and A.R. Currie. 1972. Apoptosis: a basic biological phenomenon with wide-ranging implications in tissue kinetics. *Br. J. Cancer*. 26:239-257.

Krieser, R.J., K.S. MacLea, D.S. Longnecker, J.L. Fields, S. Fiering, and A. Eastman. 2002. Deoxyribonuclease IIa is required during the phagocytic phase of apoptosis and its loss causes lethality. *Cell Death Differ*. 9:956-962.

Kroemer, G., L. Galluzzi, P. Vandenabeele, J. Abrams, E.S. Alnemri, E.H. Baehrecke, M.V. Blagosklonny, W.S. El-Deiry, P. Golstein, D.R. Green, M. Hengartner, R.A. Knight, S. Kumar, S.A. Lipton, W. Malorni, G. Nunez, M.E. Peter, J. Tschopp, J. Yuan, M. Piacentini, B. Zhivotovsky, and G. Melino. 2009. Classification of cell death: recommendations of the Nomenclature Committee on Cell Death 2009. *Cell Death Differ*. 16:3-11.

Krysko, D.V., G. Denecker, N. Festjens, S. Gabriels, E. Parthoens, K. D'Herde, and P. Vandenabeele. 2006. Macrophages use different internalization mechanisms to clear apoptotic and necrotic cells. *Cell Death Differ*. 13:2011-22.

Kuida, K., T.F. Haydar, C.Y. Kuan, Y. Gu, C. Taya, H. Karasuyama, M.S. Su, P. Rakic, and R.A. Flavell. 1998. Reduced apoptosis and cytochrome

c-mediated caspase activation in mice lacking caspase 9. *Cell*. 94:325-337.

Laird, P.W., A. Zijderveld, K. Linders, M.A. Rudnicki, R. Jaenisch, and A. Berns. 1991. Simplified mammalian DNA isolation procedure. *Nucleic Acids Res.* 19:4293.

Lindsten, T., A.J. Ross, A. King, W.X. Zong, J.C. Rathmell, H.A. Shiels, E. Ulrich, K.G. Waymire, P. Mahar, K. Frauwirth, Y. Chen, M. Wei, V.M. Eng, D.M. Adelman, M.C. Simon, A. Ma, J.A. Golden, G. Evan, S.J. Korsmeyer, G.R. MacGregor, and C.B. Thompson. 2000. The combined functions of proapoptotic Bcl-2 family members bak and bax are essential for normal development of multiple tissues. *Mol. Cell*. 6:1389-99.

Marsden, V.S., L. O'Connor, L.A. O'Reilly, J. Silke, D. Metcalf, P.G. Ekert, D.C. Huang, F. Cecconi, K. Kuida, K.J. Tomaselli, S. Roy, D.W. Nicholson, D.L. Vaux, P. Bouillet, J.M. Adams, and A. Strasser. 2002. Apoptosis initiated by Bcl-2-regulated caspase activation independently of the cytochrome c/Apaf-1/caspase-9 apoptosome. *Nature*. 419:634-7.

Matsuki, Y., H.G. Zhang, H.C. Hsu, P.A. Yang, T. Zhou, C.H. Dodd, F. Cecconi, P. Gruss, T. Tadakuma, and J.D. Mountz. 2002. Different role of Apaf-1 in positive selection, negative selection and death by neglect in foetal thymic organ culture. *Scand. J. Immunol.* 56:174-84.

Muller, U., U. Steinhoff, L.F. Reis, S. Hemmi, J. Pavlovic, R.M. Zinkernagel, and M. Aguet. 1994. Functional role of type I and type II interferons in antiviral defense. *Science*. 264:1918-21.

Nagata, S. 1997. Apoptosis by death factor. *Cell*. 88:355-65.

Nagata, S. 2005. DNA degradation in development and programmed cell death. *Annu. Rev. Immunol.* 23:853-75.

Okamoto, H., H. Shiraishi, and H. Yoshida. 2006. Histological analyses of normally grown, fertile Apaf1-deficient mice. *Cell Death Differ*. 13:668-71.

Ravichandran, K.S., and U. Lorenz. 2007. Engulfment of apoptotic cells: signals for a good meal. *Nat Rev Immunol*. 7:964-74.

Reddien, P.W., and H.R. Horvitz. 2004. The engulfment process of programmed cell death in caenorhabditis elegans. *Annu. Rev. Cell Dev. Biol.* 20:193-221.

Rodewald, H.R., P. Moingeon, J.L. Lucich, C. Dosiou, P. Lopez, and E.L. Reinherz. 1992. A population of early fetal thymocytes expressing Fc gamma RII/III contains precursors of T lymphocytes and natural killer cells. *Cell*. 69:139-50.

Strasser, A., L. O'Connor, and V.M. Dixit. 2000. Apoptosis signaling. *Annu. Rev. Biochem.* 69:217-45.

Surh, C.D., and J. Sprent. 1994. T-cell apoptosis detected *in situ* during positive and negative selection in the thymus. *Nature*. 372:100-103.

Thomaidou, D., M.C. Mione, J.F. Cavanagh, and J.G. Parnavelas. 1997. Apoptosis and its relation to the cell cycle in the developing cerebral cortex. *J Neurosci*. 17:1075-85.

Vaux, D.L., and S.J. Korsmeyer. 1999. Cell death in development. *Cell*. 96:245-254.

Verney, C., T. Takahashi, P.G. Bhide, R.S. Nowakowski, and V.S. Caviness, Jr.

2000. Independent controls for neocortical neuron production and histogenetic cell death. *Dev. Neurosci.* 22:125-38.

Wei, M.C., W.X. Zong, E.H. Cheng, T. Lindsten, V. Panoutsakopoulou, A.J. Ross, K.A. Roth, G.R. MacGregor, C.B. Thompson, and S.J. Korsmeyer. 2001. Proapoptotic BAX and BAK: a requisite gateway to mitochondrial dysfunction and death. *Science*. 292:727-30.

Wu, Y.C., G.M. Stanfield, and H.R. Horvitz. 2000. NUC-1, a Caenorhabditis elegans DNase II homolog, functions in an intermediate step of DNA degradation during apoptosis. *Genes Dev.* 14:536-548.

Yoshida, H., Y.Y. Kong, R. Yoshida, A.J. Elia, A. Hakem, R. Hakem, J.M. Penninger, and T.W. Mak. 1998. Apaf1 is required for mitochondrial pathways of apoptosis and brain development. *Cell*. 94:739-750.

Yoshida, H., Y. Okabe, K. Kawane, H. Fukuyama, and S. Nagata. 2005. Lethal anemia caused by interferon-beta produced in mouse embryos carrying undigested DNA. *Nat. Immunol.* 6:49-56.

Zwart, B., C. Ciurana, I. Rensink, R. Manoe, C.E. Hack, and L.A. Aarden. 2004. Complement activation by apoptotic cells occurs predominantly via IgM and is limited to late apoptotic (secondary necrotic) cells. *Autoimmunity*. 37:95-102.

業績一覧

学術論文
1. <u>Akiomi Nagasaka</u>, Kohki Kawane, Hiroki Yoshida, Shigekazu Nagata
　　Apaf-1-dependent and independent cell death in mouse development　投稿直前

 2. <u>Akiomi Nagasaka</u>, Kohki Kawane, Nobuhiko Yamamoto, Masato Koike, Yasuo
　　Uchiyama, Shigekazu Nagata
　　Programmed cell death in the mouse brain revealed by DNase II-null mice
　　投稿準備中

3. Nakahara M, <u>Nagasaka A,</u> Koike M, Uchida K, Kawane K, Uchiyama Y, Nagata S
　　Degradation of nuclear DNA by DNase II-like acid DNase in cortical fiber cells of
　　mouse eye lens.　FEBS J. 2007; Jun; 274(12):3055-64**.**

学会
1.<u>Akiomi Nagasaka</u>, Kohki Kawane, Shigekazu Nagata

　Detection of apoptotic cells in DNaseII KO mice during developmental stages of

　mice.

（DNaseII 欠損マウスを用いたマウスの発生段階におけるアポトーシス細胞の検出）

　2008 年 12 月10日　日本分子生物学会年会